

Critical conditions for flame acceleration in long channels closed at their ignition end

Vadim N. Kurdyumov^{a,*}, Moshe Matalon^b

^aDepartment of Energy, CIEMAT, Avda. Complutense 40, 28040 Madrid, Spain

^bDepartment of Mechanical Science and Engineering, University of Illinois at Urbana-Champaign, Urbana, IL 61801, USA

Abstract

The propagation of premixed flames in long channels is investigated when a combustible mixture is ignited at one end, which is retained closed thereafter, leaving the other end open to atmospheric pressure. This constraint conditions the flow produced by gas expansion near the flame. The burned gas trapped between the flame and the closed end comes eventually to rest, while the flow sets in the fresh mixture escapes freely at the far end of the channel. Seeking for traveling wave solutions, we find that two possible solutions, corresponding to slow and fast steadily propagating flames, exist under appropriate conditions. The critical conditions are determined when the two solutions merge, and depend on the channel width, the heat release and the Lewis number. Beyond criticality, steadily propagating flames in channels closed at their ignition end are not possible. Numerical simulation of the time-dependent equations in sufficiently long channels confirm the existence of a steady propagation mode, always corresponding to the slow flame solution. Beyond criticality, the flame always accelerates as it travels down the channel.

Keywords: Flame acceleration, Flames in channels, Wall friction, Thermal expansion

1. Introduction

There has been a continuous interest in the study of flame propagation in channels or tubes, because of its fundamental importance to combustion science, on one hand, and its application to micro propulsion devices and engineering safety and reliability, on the other. Early studies [1, 2] have recognized that the boundary conditions imposed at the end of the channel have a significant effect on the flame propagation. Thus, propagation in channels open at both ends, differ from propagation from a close to an open end, or from an open towards a close end.

We have recently examined the dynamics of flame propagation in long two-dimensional adiabatic channels, open at both ends. Under such conditions, the gas is allowed to escape the channel freely and the pressure at both ends is nearly constant and equal to the ambient (atmospheric) pressure p_{atm} . In narrow channels, of width h smaller than the laminar flame thickness δ_T , the flame accelerates throughout the combustible mixture at

a nearly constant rate [3]. In wider channels, such that h is comparable, or is a multiple of the laminar flame thickness, the flame accelerates at a constant rate during an initial period that follows ignition [4]. Once it reaches a critical distance, the flame acceleration rate increases rapidly, in a near-explosion fashion. The critical conditions marking the transition for constant to rapid acceleration were found to depend on the channel width $a = h/\delta_T$. This work substantiated Shelkin's idea [5] that flame acceleration results from the combined effects of wall friction and thermal expansion. Indeed, it was demonstrated that the curved flame that results due to the resistance exerted on the gas at the walls, is further stretched by the effect of gas expansion and thus propagates at an increasing faster rate.

In this paper we examine the dynamics of flame propagation in a channel close at the ignition end. Our focus, in particular, is on the necessary conditions for the existence of steadily propagating flame solutions. They are determined by the fact that, although the gas escapes freely at the open far end, it must come to rest near the closed end of the channel where it has initiated. Beyond criticality, the flame will necessarily accelerate after reaching a certain distance down the channel. Indeed, flame acceleration from a closed end channel has

*Corresponding author

Email addresses: vadim.k@ciemat.es (Vadim N. Kurdyumov), matalon@illinois.edu (Moshe Matalon)

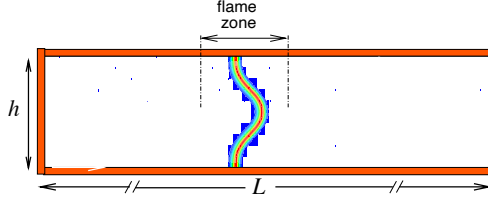


Figure 1: Schematic of the channel configuration, illustrating the various length scales associated with the flame propagation; the channel is closed at $x = 0$ and remains open at the far right.

been studied previously using model equations [6], and time-dependent numerical simulations [7, 8, 9]. These studies, however, did not recognize the possibility of steady flame propagation from a close end channel, nor were they able to identify the exact critical conditions for flame acceleration.

2. General formulation

A combustible mixture contained in a channel of length L and width h is ignited at its left end, which is retained closed as the flame propagates towards the other open end, as shown schematically in Fig. 1. The channel is considered sufficiently long, such that $L \gg h$ and the walls are assumed adiabatic and non-catalytic. The chemistry is modeled by a global, one step, irreversible reaction of the form *Fuel + Oxidizer* \rightarrow *Products* that proceeds at a rate proportional to the product of the reactant concentrations $\sim \rho^2 Y_F Y_O$, where ρ is the mixture density and Y_F, Y_O the mass fractions of the fuel and oxidizer, and an Arrhenius temperature dependence with activation energy E and a pre-exponential factor \mathcal{B} . Below, we assume that the mixture is lean in fuel and denote its mass fraction by Y for simplicity, and treats the oxidizer mass fraction as constant absorbed in \mathcal{B} .

We introduce dimensionless variable (for clarity, dimensional values are denoted here with a “prime”) as follows:

$$\begin{aligned} x &= \frac{x'}{\delta_T}, \quad y = \frac{y'}{h} = \frac{y'}{a\delta_T}, \quad t = \frac{t'}{t'_\tau} = \frac{S_L t'}{\delta_T}, \\ u &= \frac{u'}{S_L}, \quad v = \frac{v'}{aS_L}, \quad \rho = \frac{\rho'}{\rho_u}, \quad p = \frac{p' - p_{\text{atm}}}{\rho_u S_L^2 / a^2}, \\ \theta &= \frac{T' - T_u}{T_a - T_u}, \quad Y = \frac{Y'}{Y_u}, \end{aligned} \quad (1)$$

where x, y are the axial and transverse coordinates and u, v the corresponding velocity components, p is the pressure and t represents time. The density and temperature of the mixture are scaled with respect to their values in the fresh, unburned gas, denoted by the subscript “ u ”, and normalized variables have been introduced for the fuel mass fraction Y and the temperature;

the latter, denoted by θ , varies from zero in the unburned gas to one when the temperature reaches the adiabatic flame temperature $T_a = T_u + QY_u/c_p$, where Q here is the total heat release and c_p the specific heat at constant pressure. Axial distances are measured in terms of the diffusion length $\delta_T = \mathcal{D}_T/S_L$, with \mathcal{D}_T the thermal diffusivity of the mixture and S_L the laminar flame speed, while transverse distances are measured with respect to the width of the channel h . We recall that the parameter $a = h/\delta_T = O(1)$.

The dimensionless governing equations are

$$\begin{aligned} \rho(u_t + uu_x + vu_y) &= -a^{-2}p_x + Pr[a^{-2}u_{yy} \\ &\quad + \frac{4}{3}u_{xx} + \frac{1}{3}v_{xy}], \\ \rho(v_t + uv_x + vv_y) &= a^{-4}p_y + Pr[a^{-2}(\frac{4}{3}v_{yy} \\ &\quad + \frac{1}{3}u_{xy}) + v_{xx}], \\ \rho(\theta_t + u\theta_x + v\theta_y) &= \theta_{xx} + a^{-2}\theta_{yy} + \omega, \\ \rho(Y_t + uY_x + vY_y) &= Le^{-1}[Y_{xx} + a^{-2}Y_{yy}] - \omega, \\ \rho &= 1/(1 + \gamma\theta). \end{aligned} \quad (2)$$

where subscripts denote partial differentiation. The parameter $\gamma = (T_a - T_u)/T_u$ is the heat release parameter, $Le = \mathcal{D}_T/\mathcal{D}_F$ is the Lewis number, with \mathcal{D}_F the molecular diffusivity of the fuel, and $Pr = \nu/\mathcal{D}_T$ is the Prandtl number, with ν the kinematic viscosity of the mixture. The reaction rate ω is given by

$$\omega = \frac{\beta^2(1 + \gamma)^2}{2Le s_L^2} \rho^2 Y \exp\left\{\frac{\beta(\theta - 1)}{(1 + \gamma\theta)/(\gamma + 1)}\right\}, \quad (3)$$

where $\beta = E(T_a - T_0)/\mathcal{R}T_a^2$ is the Zel'dovich number. In writing (3), the approximate expression for the laminar flame speed,

$$S_{L,\text{asp}} = \sqrt{2\rho_u Le \mathcal{D}_{th} \mathcal{B}/\beta^2 (T_u/T_a)} e^{-E/2\mathcal{R}T_a} \quad (4)$$

valid for $\beta \rightarrow \infty$, was used, and an adjustment factor $s_L = S_L/(S_{L,\text{asp}})$ was introduced to ensure that for a finite β , the flame speed S_L takes on the correct (numerical) value. The numerical value of s_L , for a given β and Le , is determined as the eigenvalue of the one-dimensional planar adiabatic flame problem, as discussed in [3]. These equations must be solved subject to the following boundary conditions

$$\begin{aligned} u = v = \theta_y = Y_y &= 0 && \text{along } y = 0, 1; \\ u = v = \theta - 1 = Y &= 0 && \text{at } x = 0; \\ p = v = \theta = Y - 1 &= 0 && \text{at } x = \ell, \end{aligned} \quad (5)$$

where $\ell = L/\delta_T$ is the dimensionless channel length.

3. Steadily propagating flames - the eigenvalue problem

Seeking traveling wave solutions in sufficiently long channels, $\ell \gg 1$, we introduce the flame-attached coor-

dinate $\xi = x - \dot{x}_f t$, where \dot{x}_f is the (constant) propagation speed that remains to be determined. The governing equations (2) reduce to

$$\begin{aligned} & [\rho(u - \dot{x}_f)]_\xi + (\rho v)_y = 0 \\ & \rho(u - \dot{x}_f)u_\xi + \rho v u_y = -a^{-2}p_\xi + Pr[a^{-2}u_{yy} \\ & \quad + \frac{4}{3}u_{\xi\xi} + \frac{1}{3}v_{\xi y}] \\ & \rho(u - \dot{x}_f)v_\xi + \rho v v_y = -a^{-4}p_y + Pr[a^{-2}(\frac{4}{3}v_{yy} \\ & \quad + \frac{1}{3}u_{\xi y}) + v_{\xi\xi}] \\ & \rho(u - \dot{x}_f)\theta_\xi + \rho v \theta_y = \theta_{\xi\xi} + a^{-2}\theta_{yy} + \omega \\ & \rho(u - \dot{x}_f)Y_\xi + \rho v Y_y = Le^{-1}[Y_{\xi\xi} + Y_{yy}] - \omega \end{aligned} \quad (6)$$

and their solution must match the flow in the far field, as $\xi \rightarrow \pm\infty$. The latter are described by

$$p_y = 0, \quad p_\xi = Pr u_{yy},$$

as discussed in [4], and constitute Poiseuille flows given by $u = 6U^\pm y(1 - y)$ where U^\pm denote the mean gas velocity ahead/behind the flame that remain to be determined. The pressure is obtained a-posteriori from $p_\xi = -12Pr U^\pm$. The matching conditions are, therefore,

$$\begin{aligned} u & \sim 6U^\pm y(1 - y), \quad v \sim 0 & \text{as } \xi \rightarrow \pm\infty \\ \theta & \sim 0, \rho \sim 1, Y \sim 1 & \text{as } \xi \rightarrow +\infty \\ \theta & \sim 1, \rho \sim (1 + \gamma)^{-1}, Y \sim 0 & \text{as } \xi \rightarrow -\infty. \end{aligned} \quad (7)$$

For steady propagation, a relation between U^+ and U^- can be obtained by integrating the mass conservation equation with respect to ξ , from $-\infty$ to $+\infty$. One finds

$$(1 + \gamma)[U^+ - \dot{x}_f] = [U^- - \dot{x}_f] \quad (8)$$

Thus, for a given value of U^+ , the set of equations (6), the boundary conditions along the walls (5) and the matching conditions (7) constitute an eigenvalue problem for the determination of the propagation speed \dot{x}_f . The position of the flame front x_f is defined as the location where the reaction rate ω reaches its maximum value along the mid-plane (due to the imposed symmetry) and the propagation speed \dot{x}_f is subsequently determined by direct differentiation. The solution of this eigenvalue problem, may be expressed in the form $U^+ = \mathcal{F}(\dot{x}_f)$, where the functional dependence on the eigenvalue \dot{x}_f appearing on the right hand side is determined numerically. Substituting into (8) yields

$$U^- = (1 + \gamma)\mathcal{F}(\dot{x}_f) - \gamma\dot{x}_f. \quad (9)$$

In a narrow channels, $a \ll 1$, all variables except for the flow velocity u are, to leading order, independent of y . Integrating the mass conservation equation across the channel yields $\rho(U - \dot{x}_f) = C$, where U is the mean flow velocity, and the constant $C = -1$ by direct

comparison to the classical one-dimensional eigenvalue problem of a planar adiabatic flame; see also [3]. Then, $U^+ = \dot{x}_f - 1$ implying that $\mathcal{F}(\dot{x}_f)$ is a linear function of \dot{x}_f , or $\mathcal{F}(\dot{x}_f) = \dot{x}_f - 1$. Consequently $U^- = \dot{x}_f - (1 + \gamma)$ is also a linear function of \dot{x}_f .

In general, i.e., for $a = O(1)$, the functional dependence $\mathcal{F}(\dot{x}_f)$ must be determined numerically. The numerical methodology for solving the eigenvalue problem has been discussed in [4] and will not be repeated here. In all the calculations reported below, we have fixed $\beta = 10$ and $Pr = 0.72$ and examined the dependence of the propagation speed on the channel width a , the heat release parameter γ , and Lewis number Le .

The dependence of U^+ and of U^- on \dot{x}_f are shown in Fig. 2 for $Le = 1$, $\gamma = 5$ and selected values of a . The analytical linear dependence for $a \ll 1$ is shown by the dashed lines. It is remarkable that the linear dependence remains valid for a as large as $a = 5$, provided U^+ is not too large. It is particularly important to note the multi-valuedness of U^- , the consequence of which will be discussed below.

Consider first the general case of a flame propagating in a channel with a *prescribed flow*, of mean velocity U^+ , with the flow of the burned gas U^- given by (9). The flame propagates in the direction of the flow, when $U^+ > 0$ and against the flow when $U^+ < 0$, the latter corresponds to flame flashback. The case of the flame propagation to close end is obtained when $U^+ = 0$. The results are similar to those reported in [10, 11] for constant density flows. One can see that for any U^+ there is a unique propagation speed \dot{x}_f .

4. Steady propagation from a closed to an open end

For self propagating flames in a channel retained closed at the ignition end, the boundary conditions at $x = 0$ yields $U^- = 0$, implying that the expanding gas that moves initially away from the flame, in an opposite direction to its propagation, comes eventually to rest. Then Eq. (9), or equivalently the intersection of the curves in Fig. 2(b) with the abscissa, determines the propagation speed uniquely. The mean flow U^+ and, consequently, the flow field in the unburned gas is determined from Eq. (8). The analytical solution for $a \ll 1$ implies that in narrow channels $\dot{x}_f = 1 + \gamma$, in analogy with spherically expanding flames of sufficiently large radii [12].

Figure 2(b) shows that for sufficiently small values of a there are two possible solutions for \dot{x}_f , marked with the symbols \circ and \bullet in the figure. The lowest value of the two, which tends to the analytical solution as $a \rightarrow 0$,

is presumably the one that will be observed experimentally, as further substantiated below. The two solutions approach each other as a increases, and merge when $a = a_c$; the critical value $a_c = 5.36$ for $Le = 1$ and $\gamma = 5$. For $a > a_c$, the curve U^- no longer intersects the abscissa, implying that in sufficiently wide channels steady propagation solutions are not possible.

The flame structure and the flow field corresponding to the two distinct steady propagating solutions, for a channel width $a = 5$, are shown in Fig. 3. The color

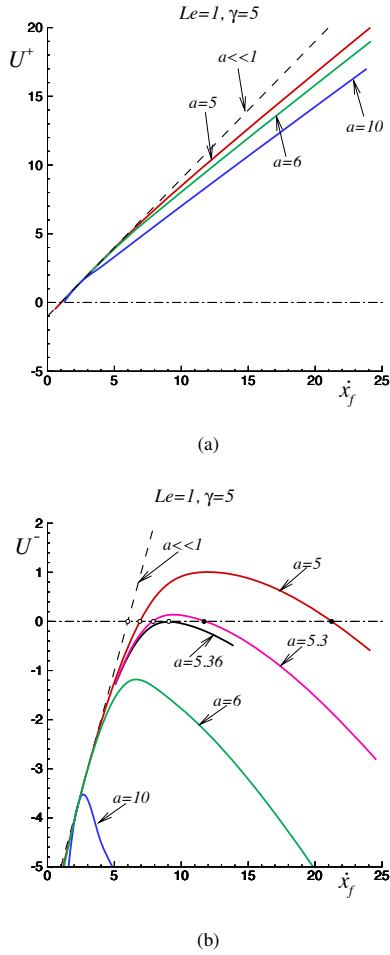


Figure 2: The mean velocity U^+ ahead, and U^- behind the flame as a function of the propagation speed \dot{x}_f , resulting from the solution of the eigenvalue problem (6). The dashed lines are the analytical results for $a \ll 1$. The symbols \circ and \bullet , at the intersection of U^- with the abscissa in figure (b), mark the two possible steady propagating flame solutions.

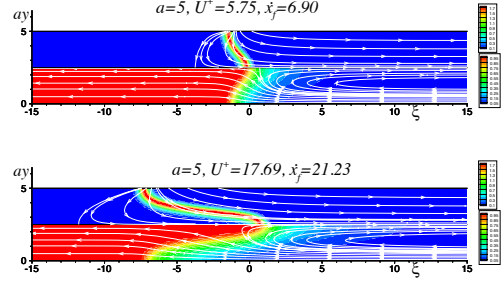


Figure 3: Illustration of the flame structure and flow field of the two distinct steadily propagating solutions, in a channel of width $a = 5$ closed at the ignition (left) end.

shades in the upper part of the channel correspond to variations in the reaction rate ω , which is clearly negligible on either side of the flame. The color shades in the lower part of the channel correspond to variations in temperature and, indeed, in the temperature in the burned gas region (on the left) is the adiabatic flame temperature and in the fresh mixture (on the right) is the temperature of the fresh mixture. The flame shape, and the extent of the reaction zone, are clearly identified by the reaction rate contours in the upper part of the channel, while the extent of the preheat zone is visualized by the temperature spread away from the flame in the lower part of the channel. The flow field is illustrated by streamlines drawn relative to walls in the upper part of the channel, and relative to an observer moving with the flame in the bottom part of the channel. It is evident that at a sufficiently large (compared to the flame thickness) distances from the flame, the induced flow in the unburned gas is parallel to the walls while the flow of the burned gas is at rest.

The dependence of U^- on \dot{x}_f is plotted in Fig. 4 for $\gamma = 5$ and two different values of Lewis number, similar to Fig. 2(b) corresponding to $Le = 1$. Although when $a \ll 1$ the solution is independent of the Lewis number, in wider channels the critical a_c increases with increasing Le implying that larger Lewis number mixtures can more easily propagate steady flames. The channel width, below which steady propagation is not possible, is reduced from $a_c = 8.64$ when $Le = 1.2$, to $a_c = 5.36$ when $Le = 1$, and $a_c = 3.75$ when $Le = 0.7$. The propagation speed at criticality reduces only slightly, from $\dot{x}_f = 11.3$ when $Le = 1.2$ to $\dot{x}_f = 7.5$ when $Le = 0.7$. The dependence of the critical a_c on the Lewis number, for $\gamma = 5$, is shown in Fig. 4(a), where steady propagation is not possible for parameter values above the curve (i.e., low Le flames). Note, in particular, the

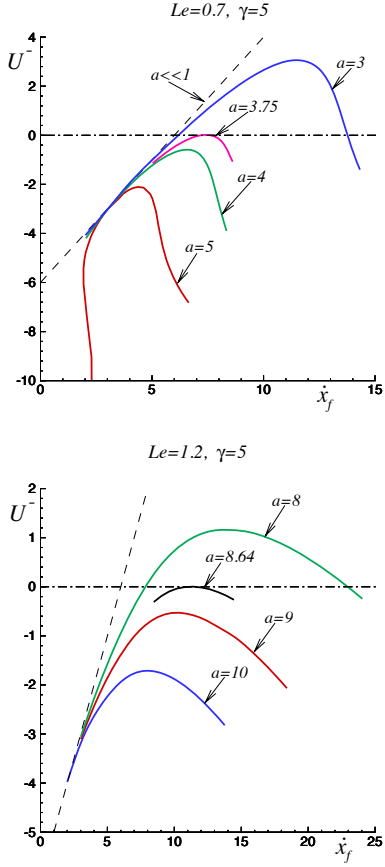
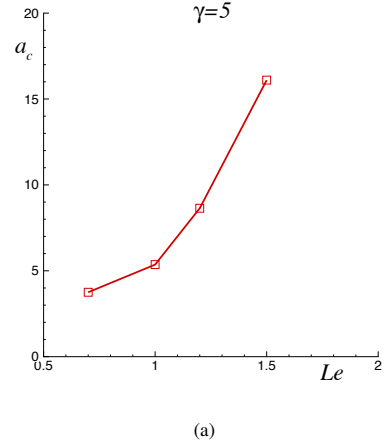


Figure 4: The mean velocity U^- behind the flame as a function of the propagation speed \dot{x}_f , for two values of the Lewis number.

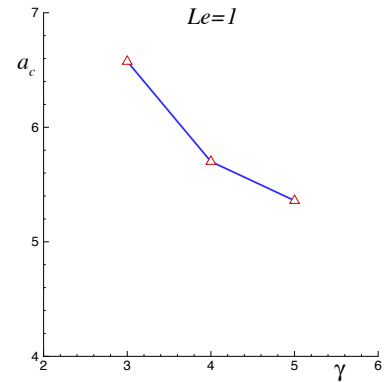
sharp increase in a_c for $Le > 1$ implying, for example, that in rich hydrogen-air flames, for which $Le \approx 2$ for an equivalence ratio $\phi = 2$ [13], steady propagation will be possible in channels twenty times wider than the flame thickness. In Fig. 4(b) we show the dependence of the critical a_c on the heat release parameter, for a fixed $Le = 1$, implying that steady propagation is not possible for sufficiently large values of γ .

5. Steady propagation vs flame acceleration

To substantiate the aforementioned results, the time-dependent problem (2) was addressed for the two different values, $a = 5$ and $a = 6$ lying below and above the critical value a_c , in a sufficiently long channel of length $\ell = 100$, with $\gamma = 5$ and $Le = 1$. We anticipate



(a)



(b)

Figure 5: Dependence of (a) the Lewis number Le and (b) the heat release parameter γ , on the critical value a_c . Steady propagation is only possible below the curves.

that independent of the initial conditions the flame, after an initial transient, will propagate steadily in a channel of width $a = 5$, but not in the channel with $a = 6$. For the latter, the solution of the time-dependent problem will illustrate the nature of the propagation. The numerical simulations were carried out using the time-marching procedure proposed in [14], with the velocity vector decomposed into irrotational and solenoidal components and solved respectively by introducing potential and stream-like functions. The initial conditions adopted correspond to a hot spot near the close (left) end of the channel, in a mixture that is otherwise at rest.

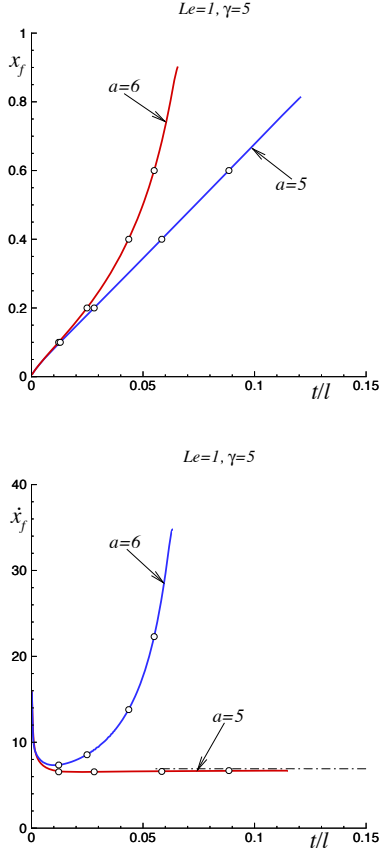


Figure 6: The flame position (in units of L) and the propagation speed (in units of S_L) plotted as a function of time in a finite length channel $\ell = 100$, for $\gamma = 5$ and $Le = 1$. The symbols \circ identify the selected times used in Figs. 7 to illustrate the flame structure and position.

Figure 6 shows the dependence of the flame position x_f , scaled with respect to ℓ , and propagation speed \dot{x}_f on time. The effect of the energy deposited as an initial condition is seen to fade away after a short time interval. Indeed, when $a = 5$, the flame speed approaches the constant value predicted in the previous section and shown by a dash-dotted line in the figure. When $a = 6$, the flame speed increases continuously as the flame accelerates towards the open end of the channel.

Figure 7 shows the propagating flames (in the lower half of the channel) at different times for the two cases under consideration. Note that the x -axis has been shifted to adjust the flame position within the frame of the graph. The snapshots correspond to the points marked by the symbol \circ in Fig. 6. We note that un-

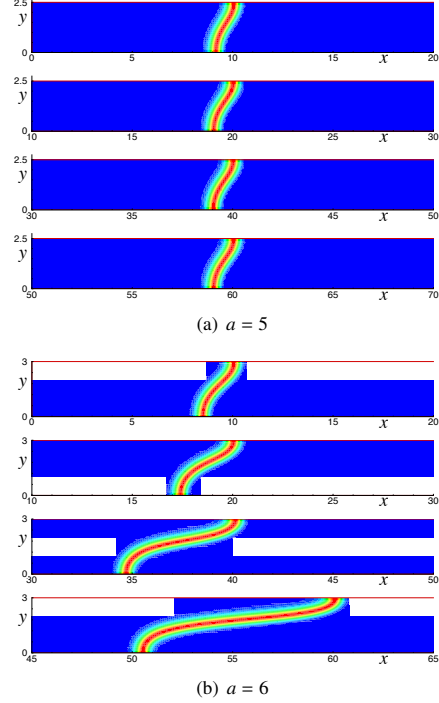


Figure 7: Illustration of the flame structure and position based on the numerical simulations of flame propagation in a channel of length $\ell = 100$. Shown are selected reaction rate contours in the lower half of the channel at different times, corresponding to the positions marked by \circ in Fig. 6.

like the steadily propagating flame, the flame structure of the accelerating flame changes continuously in time. Stretching out for additional fuel, the flame under the combined effects of friction and thermal expansion becomes further elongated during its acceleration, similar to our results on flame propagation in channels open at both ends [4].

Figures 8 and 9 shows the axial pressure and velocity profiles for the two cases under consideration at selected times (the first four, correspond to the times selected in the illustration of Fig. 7). When the flame propagates steadily (as for $a = 5$), the burned gas trapped between the flame and the end of the channel remains at rest while the pressure level decreases in time. The constant pressure gradient ahead of the flame drives a flow of constant velocity towards the open end of the channel. The pressure and velocity change dramatically when the flame accelerates (as for $a = 6$) down the channel. Although the burned gas behind the flame remains at rest, the pressure builds up in time. As a consequence, the

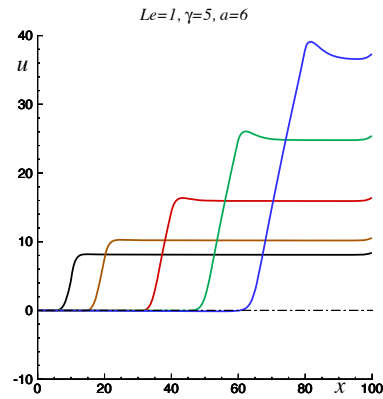
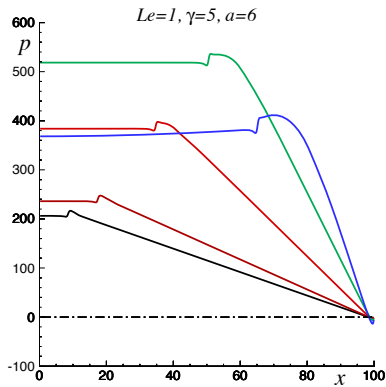
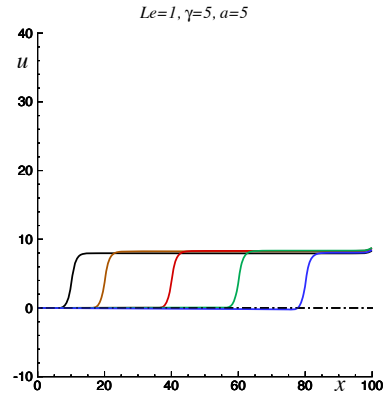
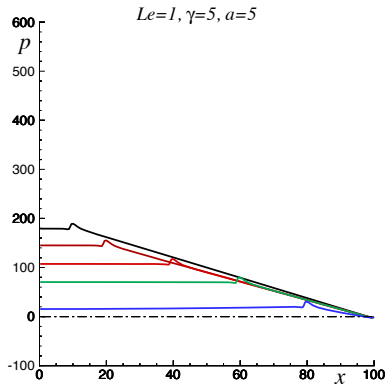


Figure 8: Pressure (along the wall) variations at selected times during the propagation in a channel of length $\ell = 100$, with $\gamma = 5$ and $Le = 1$.

Figure 9: Velocity (along the centerline) variations at selected times during the propagation in a channel of length $\ell = 100$, with $\gamma = 5$ and $Le = 1$.

constant pressure gradient developing in the unburned gas region becomes sharper and drives a flow of continuously increasing velocity near the open end of the channel. The slightly lower pressure in the last time interval may be a result of boundary effects. Measuring the velocity at the outflow may provide means to experimentally quantify the dynamics of flame propagation in channels.

6. Concluding remarks

The boundary conditions imposed at the end of a channel, within which a premixed flame is propagating, have a significant effect on the mode of propagation. Our earlier work on channels open at both ends,

has shown that the flame always accelerates when traveling down the channel. The flame acceleration is associated with the ability of the gas to escape freely from the channel. The expanding gas near the flame sets the gas in motion and creates, as a result of frictional forces, pressure gradients that drive the unburned and burned gases towards the opposite ends of the channel. Stretching out for the escaping fuel the flame moves faster. The resulting elongated flame is continuously stretched by the combined effects of friction and thermal expansion, leading to a continuous increase in propagation speed. In contrast, when the flame propagates in a channel close at the ignition end, the burned gas trapped between the flame and the end of the channel comes to rest and only the unburned gas is allowed to escape the channel

freely. As a result two modes of propagation are possible: (i) The flame, after an initial transient, propagates steadily at a speed determined by the mixture properties (heat release parameter and Lewis number) and the channel's width, and (ii) the flame after an initial transient accelerates down the channel at an ever-increasing speed. Steady propagation results in sufficiently narrow channels, when the heat release is not too large and in mixtures of sufficiently large Lewis numbers.

To the best of our knowledge, the existence of a steady mode of propagation in channels closed at their ignition end together with the existence of double velocity solutions, has not been discovered before, and this work marks the first investigation that identifies explicit conditions for the flame acceleration.

Acknowledgment

V.K. acknowledges also the support of Spanish MEC under Project Consolider-Ingenio 2010 (grant # CSD2010-00011).

7. References

- [1] E. Mallard, H. Le Chatelier, Combustion des mélanges gazeux explosifs, *Ann. Mines Série, IV* (1883) 274–388.
- [2] H. Guénoche, Flame propagation in tubes and in closed vessels, in: G. Markstein (Ed.), *Unsteady Flame Propagation*, Macmillan, 1964, pp. 107–181.
- [3] V. N. Kurdyumov, M. Matalon, Flame acceleration in long narrow open channel, *Proceedings of the Combustion Institute* 34 (2013) 865–872.
- [4] V. Kurdyumov, M. Matalon, Self accelerating flames in long narrow open channels, *Proceedings of the Combustion Institute* 35 (2015).
- [5] K. I. Shelkin, *Journal of Experimental and Theoretical Physics* (1940) 823–827.
- [6] V. Bychkov, V. Akkerman, G. Fru, A. Petchenko, L. Eriksson, Flame acceleration in the early stages of burning in tubes, *Combustion and Flame* 150 (2007) 263–276.
- [7] J. Ott, E. Oran, J. Anderson, A mechanism for flame acceleration in narrow tubes, *AIAA J.* 41 (2003) 1391–1396.
- [8] V. Gamezo, E. Oran, Flame acceleration in narrow channels: Applications for micropropulsion in low-gravity environments, *AIAA Journal* 44 (2006) 329–336.
- [9] B. Demirgok, O. Ugarte, D. Valiev, V. Akkerman, Effect of thermal expansion on flame propagation in channels with non-slip walls, *Proceedings of the Combustion Institute* 35 (2015) 929–936.
- [10] J. Daou, M. Matalon, Influence of conductive heat-losses on the propagation of premixed flames in channels, *Combustion and Flame* 128 (2002) 321–339.
- [11] V. Kurdyumov, Lewis number effect on the propagation of premixed flames in narrow adiabatic channel: Symmetric and non-symmetric flames and their linear stability analysis, *Combustion and Flame* 158 (2011) 1307–1317.
- [12] J. Bechtold, M. Matalon, Hydrodynamic and diffusion effects on the stability of spherically expanding flames, *Combustion and Flame* 67 (1987) 77.
- [13] C. E. Frouzakis, N. Fogla, A. Tomboulides, A. C., M. Matalon, Numerical study of unstable hydrogen/air flames: shape and propagation speed, *Proceedings of the Combustion Institute* 35 (2015) 1087–1095.
- [14] V. Kurdyumov, M. Matalon, Effect of thermal expansion on the stabilization of an edge-flame in a mixing-layer model, *Proceedings of the Combustion Institute* 32 (2009) 1107–1115.